International Journal of Nanomedicine

Dovepress
open access to scientific and medical research

Open Access Full Text Article

ORIGINAL RESEARCH

Rapid green synthesis of silver and gold nanoparticles using *Dendropanax morbifera* leaf extract and their anticancer activities

This article was published in the following Dove Press journal:
International Journal of Nanomedicine
10 August 2016
Number of times this article has been viewed

Chao Wang[1]
Ramya Mathiyalagan[2]
Yeon Ju Kim[1]
Veronica Castro-Aceituno[1]
Priyanka Singh[1]
Sungeun Ahn[1]
Dandan Wang[1]
Deok Chun Yang[1,2]

[1]Department of Oriental Medicine Biotechnology and Ginseng Bank, [2]Graduate School of Biotechnology and Ginseng Bank, College of Life Sciences, Kyung Hee University, Yongin, Republic of Korea

Abstract: *Dendropanax morbifera* Léveille is an oriental medicinal plant that is traditionally used in folk medicine and grows in a specific region of South Korea. We aimed to enhance the utilization of *D. morbifera* medicinal plants for synthesis of silver nanoparticles (AgNPs) and gold nanoparticles (AuNPs). *D. morbifera* leaf extract acted as both a reducing and a stabilizing agent that rapidly synthesized *Dendropanax* AgNPs (D-AgNPs) and *Dendropanax* AuNPs (D-AuNPs). The D-AgNPs and D-AuNPs were characterized by ultraviolet-visible spectroscopy, energy dispersive X-ray analysis, elemental mapping, field emission transmission electron microscopy, X-ray diffraction, and dynamic light scattering. The characterizations revealed that the D-AgNPs and D-AuNPs were in polygon and hexagon shapes with average sizes of 100–150 nm and 10–20 nm, respectively. The important outcomes were the synthesis of AgNPs and AuNPs within 1 hour and 3 minutes, respectively, avoiding the subsequent processing for removal of any toxic components or for stabilizing the nanoparticles. Additionally, D-AgNPs and D-AuNPs were examined for cytotoxicity in a human keratinocyte cell line and in A549 human lung cancer cell line. The results indicated that D-AgNPs exhibited less cytotoxicity in the human keratinocyte cell line at 100 µg/mL after 48 hours. On the other hand, D-AgNPs showed potent cytotoxicity in the lung cancer cells at the same concentration after 48 hours, whereas D-AuNPs did not exhibit cytotoxicity in both cell lines at the same concentration. However, both D-AgNPs and D-AuNPs at 50 µg/mL enhanced the cytotoxicity of ginsenoside compound K at 25 µM after 48 hours of treatment compared with CK alone. We believe that this rapid green synthesis of D-AgNPs and D-AuNPs is a valuable addition to the applications of *D. morbifera* medicinal plant. D-AuNPs can be used as carriers for drug delivery and in cancer therapy due to their lack of normal cell cytotoxicity.

Keywords: biosynthesis, silver and gold nanoparticles, *Dendropanax morbifera* leaf extract, human lung cancer, HaCaT cells, compound K

Introduction

Dendropanax plants belong to the *Araliaceae* family, which contains more than 80 different species that are mainly distributed in Eastern Asia and tropical America. *Dendropanax morbifera* (*D. morbifera*) Léveille has long been used as a traditional medicinal plant and health food in the Republic of Korea. The *D. morbifera* plants have been reported to contain acetylenes, saponin glycosides such as oleifoliosides A and oleifoliosides B,[1] dendropanoxide,[1] terpenoids,[2] and volatile oil.[3] Recent research indicates that the total volatile oil of *D. morbifera* leaves can significantly reduce total cholesterol, triglycerides, and low-density lipoprotein cholesterol levels in mice serum, as well as promote high-density lipoprotein cholesterol level in a dose-dependent manner.[4] Also, inhibitory effects of *D. morbifera* leaf extract on

Correspondence: Yeon Ju Kim; Deok Chun Yang
Department of Oriental Medicine Biotechnology and Ginseng Bank, College of Life Sciences, Kyung Hee University, Yongin 446-701, Republic of Korea
Tel +82 31 201 2100
Fax +82 31 205 2688
Email yeonjukim@khu.ac.kr; dcyang@khu.ac.kr

http://dx.doi.org/10.2147/IJN.S97181

proliferation and migration of vascular smooth muscle cells[5] and strong antioxidant effects in the hippocampus of mercury-exposed rats have been reported.[6] In addition, the plant has traditionally been used for improving blood circulation. For example, the bioflavonoid rutin demonstrates antithrombic and anticoagulant activities.[7] Although different medicinal plants have been reported for green synthesis of silver nanoparticles (AgNPs) and gold nanoparticles (AuNPs),[8,9] we utilized the leaf extract of *D. morbifera* to increase the utility of this plant.

Metal nanoparticles, especially silver and gold, have gained special attention in biomedical fields for applications, including antimicrobial agents in clothing[10,11] and anti-inflammatory agents in cosmetics,[12] in medical devices,[13] and in cancer therapy and diagnostics.[14]

In this study, we focused on the biosynthesis of *Dendropanax* AgNPs (D-AgNPs) and *Dendropanax* AuNPs (D-AuNPs) using the crude extract of *D. morbifera* Léveille leaves. This green-based method synthesized D-AgNPs and D-AuNPs that were further characterized by ultraviolet-visible (UV-vis) spectroscopy, field emission transmission electron microscopy (FE-TEM), energy dispersive X-ray analysis (EDX), elemental mapping, X-ray diffraction (XRD), and dynamic light scattering (DLS). Additionally, in vitro cytotoxic assays in human keratinocyte cell line (HaCaT) and human A459 lung cancer cells revealed that AgNPs showed less cytotoxicity in the HaCaT cell line but decreased cell viability in A459 lung cancer cells. Also, these particles increased the anticancer activity of the ginsenoside compound K (CK). However, AuNPs exhibited no cytotoxicity in any of the cell lines and enhanced the anticancer efficacy of CK. To the best of our knowledge, this is the first report on the synthesis of AgNPs and AuNPs using the leaves of *D. morbifera* Léveille.

Materials and methods

The leaves of six-year-old *D. morbifera* were purchased from Serom, Republic of Korea. Silver nitrate ($AgNO_3$) and gold (III) chloride trihydrate ($HAuCl_4 \cdot 3H_2O$) (analytical grade) were purchased from Sigma-Aldrich Co (St Louis, MO, USA). Other components and media were purchased from Difco, MB Cell (Seoul, Republic of Korea).

Preparation of leaf extract

The preparation of *Dendropanax* leaf extract followed the protocol mentioned by Singh et al.[10] Healthy leaves of *D. morbifera* were washed with deionized water, cut into small pieces, and dried. Then, 5 g of the dried leaves was transferred into 1 L of distilled water and boiled for 30 minutes, a process that extracted the leaf components into water. The extract was allowed to cool at room temperature, further centrifuged at 5,000 rpm for 10 minutes, and then filtered through Whatman filter paper (No 2) to remove any suspended particles. Finally, a clear filtrate was obtained, and the total volume of the filtrate was brought up to 100 mL and stored at 4°C for further experiments.

Biosynthesis of D-AgNPs and D-AuNPs

For the biosynthesis of AgNPs, 5 mL of leaf extract was mixed with 45 mL of deionized water, and $AgNO_3$ solution was added to a final concentration of 1 mM in the reaction mixture. The mixture was then incubated at 80°C for 1 hour. The color change in the reaction mixture was observed continuously and compared with that of the control for various periods of time as follows: 10 minutes, 20 minutes, 30 minutes, 45 minutes, and 1 hour. A similar procedure was used for the synthesis of D-AuNPs in which gold (III) chloride trihydrate was added to a final concentration of 1 mM. The reaction mixture color change was monitored at 1 minute, 2 minutes, and 3 minutes. The formed D-AgNPs and D-AuNPs were collected in the form of pellets by centrifugation at 16,000 rpm for 20 minutes and washed several times with deionized water to remove any unwanted substances. These final products were dried and used for further characterizations.

Characterization of D-AgNPs and D-AuNPs

The reaction mixtures were scanned in the range of 350–800 nm and 400–800 nm for D-AgNPs and D-AuNPs, respectively, in a UV-vis spectrophotometer (Ultrospec 2100 pro, GE Healthcare Bio-Sciences Corp., Piscataway, NJ, USA). The shape, morphology, and dispersal of the nanoparticles were analyzed by TEM and elemental mapping by EDX in a JEM-2100F (JEOL, Tokyo, Japan) instrument operated at 200 kV. This process used a carbon-coated copper grid on which one drop of D-AgNPs or D-AuNPs was placed, dried at 60°C, and observed under a TEM-EDX microscope. The size distribution profile of the synthesized nanoparticles was analyzed using DLS with a particle size analyzer (Photal, Otsuka Electronics Co., Osaka, Japan). The purities of synthesized D-AgNPs and D-AuNPs were analyzed by XRD (X-ray diffractometer D8 Advance; Bruker Optik GmbH, Ettlingen, Germany) at 40 kV, 40 mA, with Cu kα radiation, at a scanning rate of 6°/min, a step size of 0.02, over the 2θ range of 20°–80°.

In vitro cytotoxic assay in human keratinocyte cells and lung cancer cells

HaCaT cells were purchased from the American Type Culture Collection, seeded at a density of 5×10^3 cells/well

in a 96-microplate in Dulbecco's modified Eagle's medium (DMEM) (GIBCOBRL, Rockville, MD) containing 10% (v/v) fetal bovine serum (FBS) and 1% (v/v) penicillin/streptomycin (WelGENE Inc., Daegu, Korea) and incubated at 37°C in a humidified atmosphere containing 5% CO_2 and 95% air for 48 hours.

Human lung adenocarcinoma A549 cells from a Korean cell bank (Seoul, South Korea) were cultured in RPMI 1640 culture media (GenDEPOT Inc., Barker, Texas, USA) supplemented with 10% fetal bovine serum, 100 IU/mL penicillin, and 100 µg/mL streptomycin (Gibco-BRL, Gaithersburg, MD, USA) and kept at 37°C in a humidified incubator with a 5% CO_2 atmosphere. No ethical approval was sought or deemed necessary by the Kyung Hee University ethics commitee as experiments were performed on commercially available cell lines.

Cell toxicity

The viability of the cells was assessed by MTT (3-(4, 5-dimethylthiazol-2-yl)-2-5-diphenyletrazolium bromide) assay. Briefly, the cells were plated at a concentration of 1×10^5 in a 96-well plate (NEST®, New Jessey, USA). After 24 hours, the cells were subjected to the following treatment for 48 hours: D-AgNPs (1 µg/mL, 10 µg/mL, and 100 µg/mL), D-AuNPs (1 µg/mL, 10 µg/mL, and 100 µg/mL), CK (1 µM, 2.5 µM, 5 µM, 10 µM, 25 µM, and 50 µM), D-AuNPs 50 µg/mL + CK (1 µM, 2.5 µM, 5 µM, 10 µM, 25 µM, and 50 µM), and D-AgNPs 50 µg/mL + CK (1 µM, 2.5 µM, 5 µM, 10 µM, 25 µM, and 50 µM). Afterward, 10 µL of MTT (5 mg/mL) was added to each well and incubated for 3 hours. Then, media containing treatment and MTT reagent were removed by aspiration and replaced with 100 µL of Dimethyl Sulfoxide (DMSO). The plates were covered with aluminum foil and kept in an incubator for 30 minutes for dissolution of the formed formazan crystals. The amount of formazan crystals formed by viable cells was measured using a multimodel plate reader (Bio-Tek Instrument, Winooski, Vermont, USA) at a test wavelength of 570 nm and compared to a reference wavelength of 630 nm. The percentage of cytotoxicity was defined as ([absorbance of treated cells]/[absorbance of control cell] ×100). Similarly, the toxic effects of D-AgNPs and D-AuNPs on HaCaT cell viability were measured by MTT assay following the same methods.

Nuclear morphology observation

Hoechst 33258 staining was performed to detect cellular apoptosis following the manufacturer's instructions. Briefly, cells were seeded in six-well plates at 5×10^5 cells/well and incubated for 24 hours. After the application of D-AgNPs and D-AgNPs with or without CK into A549 cells for 48 hours, cells were washed twice with 1× Phosphate-buffered saline (PBS) and fixed with 3.7% (v/v) formaldehyde for 5 minutes at room temperature. Prior to staining, the cells were washed twice with 1× PBS and stained with 2 µg/mL Hoechst 33258 for 30 minutes in dark conditions at room temperature. The nuclear morphologies of the Hoechst-positive cells were observed and photographed under a fluorescence microscope (×400, Optinity, Korean Labtech, Kyonggi-do, South Korea) for further analysis.

Results and discussion

In recent years, nanoparticles, especially those of silver and gold, have gained special attention due to increases in biomedical and physiochemical applications. Since ancient times, silver has been broadly studied and used to treat microbial infections, improve wound healing without scarring,[15] and in medicinal device coatings.

Numerous plants have been utilized for the synthesis of AgNPs and AuNPs.[16] Among these, ample numbers of medicinal plants mostly used in oriental medicine have also been utilized for the biosynthesis of AgNPs and AuNPs with added advantages.[9,10] In this regard, *D. morbifera* leaves and stems have been used in oriental medicine in Korea and People's Republic of China and have been reported to have beneficial effects in numerous diseases.[7,17,18] In this study, *D. morbifera* leaves were used for the first time for the green synthesis of D-AgNPs and D-AuNPs, which were further studied for their in vitro anticancer efficacies.

Biosynthesis of D-AgNPs and D-AuNPs

The *D. morbifera* leaf extracts were directly used for D-AgNP and D-AuNP synthesis without any harmful chemical or stabilizing agents. The clear plant extracts containing $AgNO_3$ solution changed to a dark brown color within 1 hour, whereas solutions containing $HAuCl_4$ turned a dark ruby red color in 3 minutes at 80°C (Figure 1A and B). Comparatively, the control without $AgNO_3$ and $HAuCl_4$ solutions did not demonstrate any color changes. These color changes indicated that the bioreduction of Ag^+ into Ag^0 in the $AgNO_3$ solution and the reduction of Au^{3+} into Au^0 in the $HAuCl_4$ solution were accelerated by *D. morbifera* leaf extract. The color changes represent visual confirmation of the formation of the corresponding nanoparticles.[19] As previously reported,[20] the polysaccharides and phytochemicals in *D. morbifera* may be responsible for the reduction and synthesis of D-AgNPs and D-AuNPs.

The synthesis, characterization methods, and various applications of silver and gold nanomaterials using different plant extracts have previously been reviewed.[16] The D-AuNPs

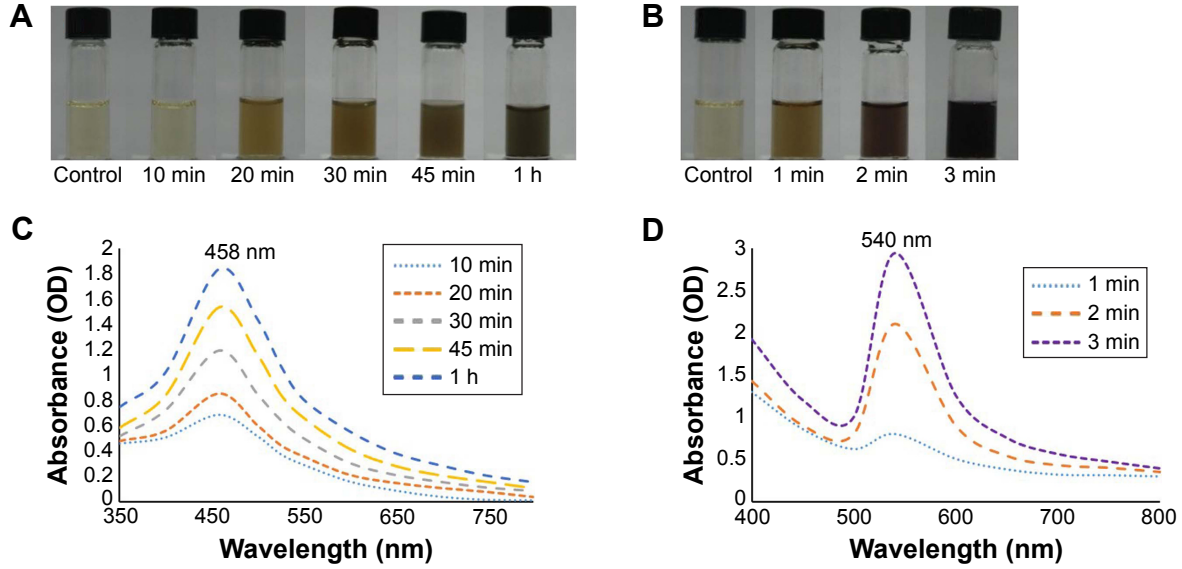

Figure 1 UV-vis spectrometry analysis of D-AgNPs and D-AuNPs formation.
Notes: Reaction mixture after incubation of *Dendropanax* leaf extract with silver nitrate ($AgNO_3$) (**A**) and gold (III) chloride trihydrate ($HAuCl_4 \cdot 3H_2O$) (**B**) at various periods of time (minutes). Time-dependent UV-vis spectra of the reaction mixture containing D-AgNPs (**C**) and D-AuNPs (**D**).
Abbreviations: UV-vis, ultraviolet-visible spectroscopy; OD, optical density; h, hours; min, minutes.

synthesis was completed within a very short time period compared to other plant extracts.[19,21] This rapid synthesis was due to the excitation of the surface plasmon resonance effect[19] and the reduction of metal ions into nanoscale particles. The time-dependent extinction of surface plasmon resonance in synthesized D-AgNP and D-AuNP solutions was indicated in UV-vis spectra (Figure 1), which exhibited characteristic bands centered at 458 nm (Figure 1C) and 540 nm (Figure 1D) for D-AgNPs and D-AuNPs, respectively, at various functions of time (min), a result which was similar to those of Singh et al's report.[9] *Dendropanax* leaf extract mediates rapid and easy synthesis of D-AgNPs and D-AuNPs compared to other leaf extracts[19,21] and bacteria-[22,23] and fungi-based syntheses.

Characterization of AgNPs and AuNPs

The morphologies and shapes of synthesized D-AgNPs and D-AuNPs were determined by FE-TEM. Figure 2A shows

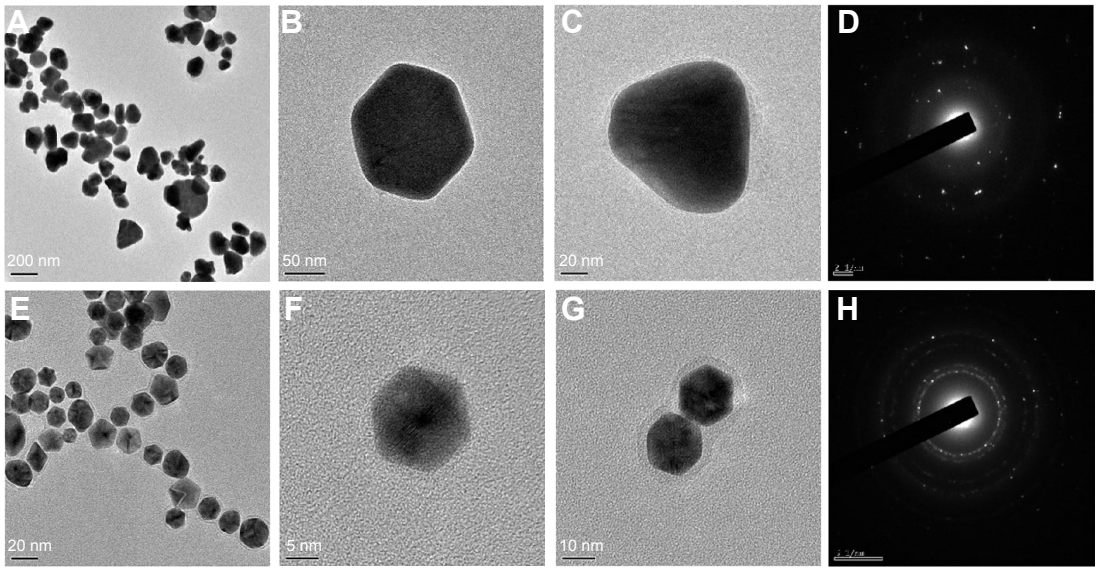

Figure 2 FE-TEM analysis of D-AgNPs and D-AuNPs.
Notes: TEM image of D-AgNPs in which the scale bar represents 200 nm (**A**), high-resolution image of a single nanocrystal at 50 nm (**B**) and 20 nm (**C**), SAED pattern (**D**). TEM image of D-AuNPs in which the scale bar corresponds to 20 nm (**E**), high-resolution image of a single nanocrystal at 5 nm (**F**) and 10 nm (**G**), and SAED pattern (**H**).
Abbreviations: TEM, transmission electron microscopy; SAED, selected area electron diffraction; D-AgNPs, *Dendropanax* silver nanoparticles; D-AuNPs, *Dendropanax* gold nanoparticles.

that the synthesized D-AgNPs were predominantly polygonal in shape, with a few hexagons and triangles. Figure 2B and C shows high-resolution lattice images of one particle with a scale bar corresponding to 50 and 20 nm, respectively. The crystalline nature of AgNPs was confirmed by the Selected area electron diffraction (SAED) pattern (Figure 2D), which contained bright circular spots corresponding to (111), (200), (220), and (311). Similarly, synthesized D-AuNPs were primarily polygonal in shape, with a few hexagon shapes, as seen in Figure 2E. Figure 2F and G shows high-resolution lattice images of one particle with a scale bar corresponding to 5 nm and 10 nm, respectively. Similar polygonal and hexagonal shapes of AgNPs and AuNPs were reported in other plant extracts,[24] which confirmed that *D. morbifera* is suitable for use in nanoparticle synthesis. The crystalline nature of AuNPs was confirmed by the SAED pattern (Figure 2H), which contained bright circular spots corresponding to (111), (200), (220), and (311). Both of the synthesized nanoparticles were monodisperse in nature, which is an added advantage of *D. morbifera*-based synthesis of nanoparticles.

Figure 3 displays the EDX spectrum of D-AgNPs and D-AuNPs using FE-TEM. Strong signals were observed at 3 keV and 2.2 keV, which correspond to the presence of elemental silver and gold, respectively, a result that was similar to Singh et al's report.[10] A weaker signal for chromium, which originates from biomolecules and certain components of *D. morbifera* leaf extract, was also found (Figure 3). Carbon and copper also produced strong signals, indicating impurities from the TEM grid used for analysis. Elemental mapping was used to determine the purity of the synthesized nanoparticles.[16] The elemental mapping results showed the distribution of AgNPs (Figure 3C) and AuNPs (Figure 3F) in the electron micrograph region.

The crystalline structures of the biosynthesized D-AgNPs and D-AuNPs were examined by XRD analysis, and the obtained patterns are shown in Figure 4. The obtained diffraction peaks at 38.19°, 44.34°, 64.48°, and 77.46° are, respectively, assigned to (111), (200), (220), and (311) lattice planes and were found to be identical to those reported for standard silver metal. For D-AuNPs, XRD peaks corresponding to four peaks with 2θ values of 38.09°, 44.40°, 64.56°, and 77.60° sets of lattice planes were observed, which indexed to the (111), (200), (220), and (311) faces of gold, respectively. These results are similar to those in a previous report.[9] Additionally, according to the XRD spectra, there were no different crystal phases on the surfaces of the D-AgNPs and D-AuNPs, indicating the absence of reduction of Ag^{+} and Au^{3+} ions with the leaf extracts of *D. morbifera*. The DLS results showed the particle size distribution of D-AgNPs and D-AuNPs according to intensity, number, and volume of nanoparticles (Figure 5). The phytochemicals and flavonoids present in the *D. morbifera* leaf extracts may have played a crucial role in the rapid synthesis of D-AgNPs and D-AuNPs. This synthesis is quite advantageous as a

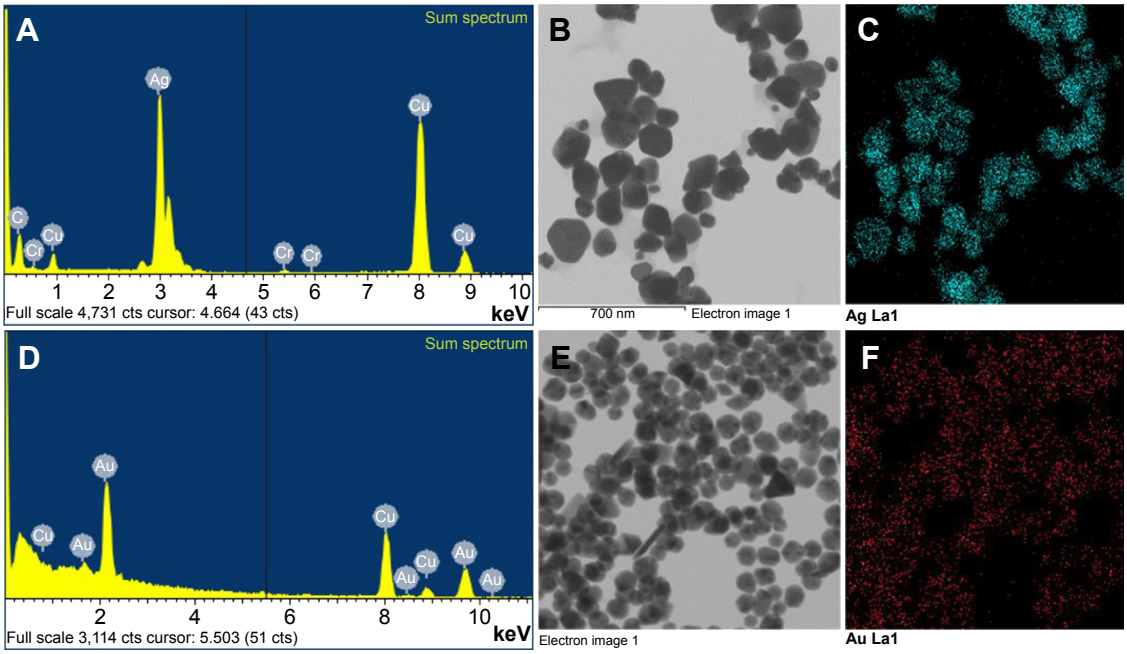

Figure 3 EDX and elemental mapping for the purity analysis of both D-AgNPs and D-AuNPs.
Notes: D-AgNPs observed in EDX spectrum (**A**), electron micrograph region (**B**), and distribution of silver in elemental mapping (**C**). D-AuNPs observed in EDX spectrum (**D**), electron micrograph region (**E**), and distribution of gold in elemental mapping (**F**).
Abbreviations: EDX, energy dispersive X-ray analysis; D-AgNPs, *Dendropanax* silver nanoparticles; D-AuNPs, *Dendropanax* gold nanoparticles.

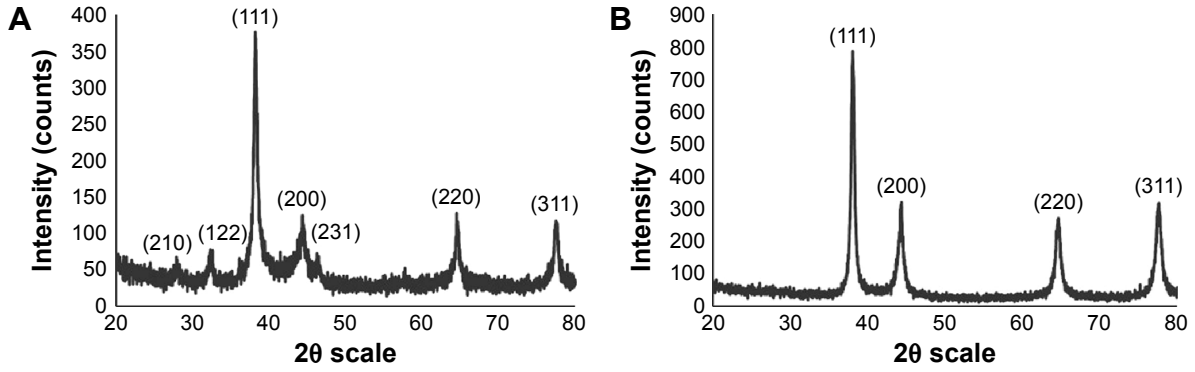

Figure 4 XRD patterns of D-AgNPs (**A**) and D-AuNPs (**B**) synthesized from *D. morbifera* leaf extract.
Abbreviations: XRD, X-ray diffraction; D-AgNPs, *Dendropanax* silver nanoparticles; D-AuNPs, *Dendropanax* gold nanoparticles; *D. morbifera, Dendropanax morbifera.*

rapid, environmentally safe, biocompatible, cost-effective, and easily scaled up mass production method.[16] Of note, the medicinal efficacy of *D. morbifera* leaves, which act as a natural treatment against several diseases such as cancer and diabetes, will create a valuable addition to the synthesis of nanoparticles and enhancement of the pharmacological activities of these nanoparticles.

Thus, our characterization studies confirm the suitability of *D. morbifera* leaves for synthesizing D-AgNPs and D-AuNPs. However, this Korean endemic tree species is

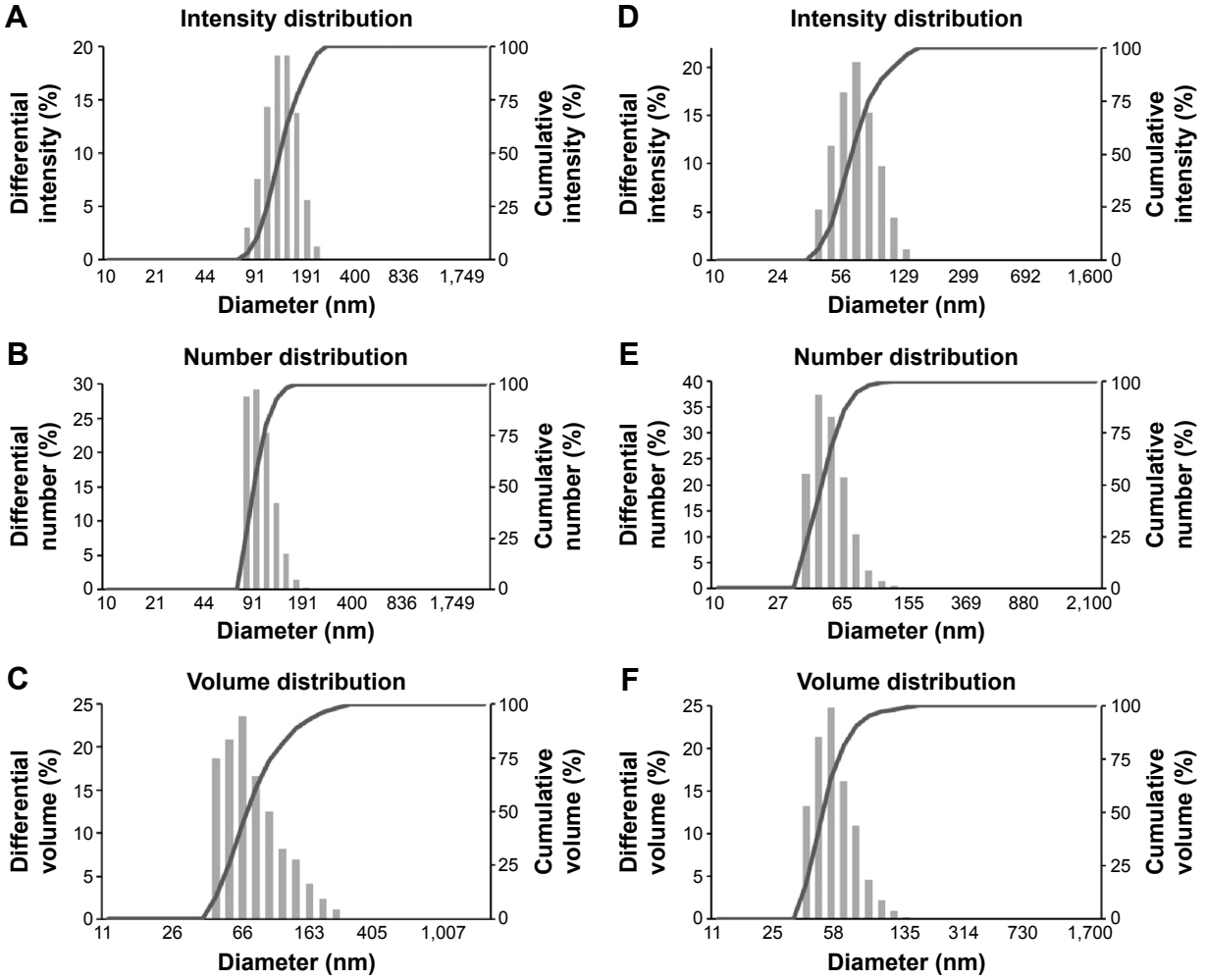

Figure 5 Particle size distribution of *D. morbifera*-mediated D-AgNPs according to intensity (**A**), number (**B**), and volume (**C**); and D-AuNPs according to intensity (**D**), number (**E**), and volume (**F**).
Abbreviations: *D. morbifera, Dendropanax morbifera*; D-AgNPs, *Dendropanax* silver nanoparticles; D-AuNPs, *Dendropanax* gold nanoparticles.

limited in its distribution, ranging from Jeju Island to Wando Island and Haenam.[25] The limited availability of *D. morbifera* is an important concern for researchers attempting to utilize this plant as a potent nanoparticle synthesizer. Continued research is needed on this topic.

In vitro cytotoxicity of D-AgNPs and D-AuNPs on HaCaT cells

For evaluating the cytotoxicity of D-AgNPs and D-AuNPs, HaCaT cell line was used in non-disease conditions for comparison. The indicated concentrations of D-AgNPs and D-AuNPs used with HaCaT cell line are shown in Figure 6. Both D-AgNPs and D-AuNPs were used at concentrations ranging from 1 µg/mL to 100 µg/mL. In addition, treatment of HaCaT cells with 10 µg/mL D-AgNPs resulted in nontoxicity to cells; however, 100 µg/mL of D-AgNPs showed less reduction in growth of cells (Figure 6A). D-AuNPs exhibited no cytotoxic effect against HaCaT cells at concentrations ranging from 1 µg/mL to 100 µg/mL (Figure 6B). These results enlightened that the D-AuNPs may not exhibit toxicity to the normal cell conditions.

In vitro cytotoxicity of D-AgNPs and D-AuNPs in lung cancer cells

Previous studies have reported the potential cell growth inhibition of various cancer cell lines by metal nanoparticles.[26,27] Lung cancer has been reported to be one of the most important causes of death worldwide.[28] In this study, A549 human lung cancer cells were used as a model to determine the cytotoxicity of D-AgNPs and D-AuNPs, as well as their synergetic effects with CK. D-AgNPs significantly inhibited A549 cell growth by more than 70% at a concentration of 100 µg/mL after 48 hours of treatment (Figure 7A). In contrast, D-AuNPs at 100 µg/mL did not induce cell toxicity after 48 hours of treatment (Figure 7B). In previous studies, the cytotoxic effects of AgNPs on cancer cells, along with the noncytotoxic effects of AuNPs, were similar to our findings.[26,27,29–31] Suliman et al reported[32] AgNPs show less cytotoxicity on A549 cell compared with D-AgNPs at same concentration. Next, the synergistic effect between *Dendropanax* nanoparticles (silver and gold) and the ginsenoside CK was determined. Ginsenoside CK is one of the important secondary metabolites of Korean Ginseng (*Panax ginseng* Meyer), which has traditionally been known as a medicinal herb in oriental medicine in Korea, People's Republic of China, and Japan. In recent years, CK (also referred as 20-*O*-(*D*-glucopyranosyl)-20(*S*)-protopanaxadiol, IH901, or compound M1) has gained special attention owing to its unique biological properties.[33–35] In our study, CK reduced cell viability to ~50% at 25 µM after 48 hours (Figure 8A). In contrast, CK decreased the cell viability to 20% at 25 µM after 48 hours when combined with D-AgNPs (Figure 8B) or D-AuNPs (Figure 8C) at 50 µg/mL. Our results suggest that D-AgNPs not only inhibit cancer cell growth but also enhance the cytotoxicity of CK in cancer cells. Due to the noncytotoxicity of D-AuNPs in cancer cells, these particles can be considered for use in drug delivery and molecular imaging techniques such as magnetic resonance imaging.[27,29] In addition, our data suggest that *Dendropanax* AuNPs increase the anticancer efficacy of CK.

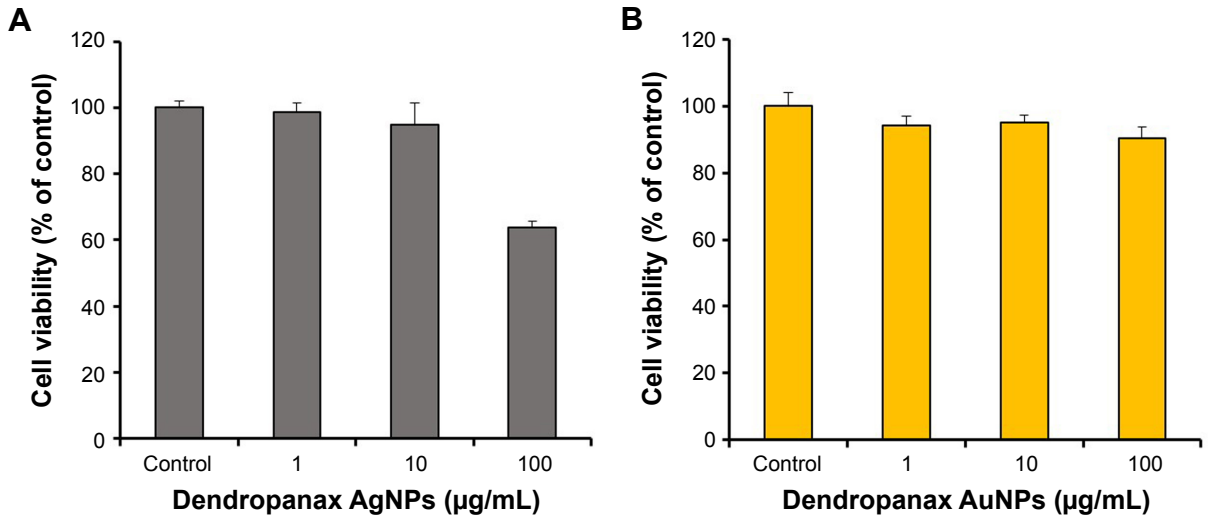

Figure 6 Effect of D-AgNPs (**A**) and D-AuNPs (**B**) on HaCaT cells.
Notes: Cells (1×10^5 cells/well) were treated with the indicated concentrations of D-AuNPs and D-AgNPs for 48 hours. Cell viability was determined with a colorimetric assay using MTT solution. Error bars represent the standard deviation (n=3).
Abbreviations: D-AgNPs, *Dendropanax* silver nanoparticles; D-AuNPs, *Dendropanax* gold nanoparticles; MTT, 3-(4, 5-dimethylthiazol-2-yl)-2-5-diphenyletrazolium bromide.

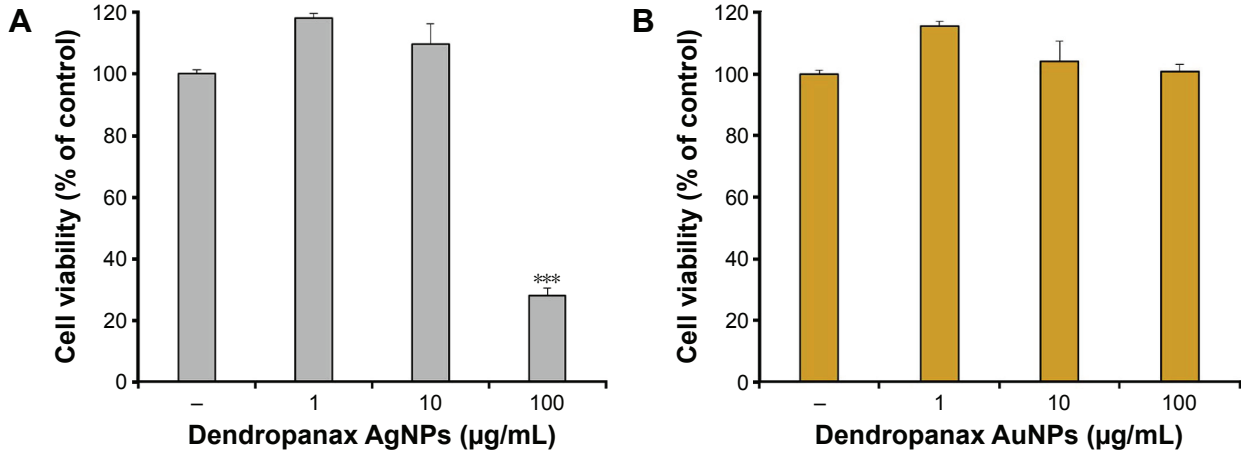

Figure 7 Dose-dependent cytotoxicity of (**A**) D-AgNPs and (**B**) D-AuNPs after 48 hours of treatment in A549 human lung cancer cells.
Notes: Error bars represent the standard deviation (n=3). ***$P<0.001$ versus control (untreated group). The statistical significance of differences between values was evaluated by one-way ANOVA.
Abbreviations: D-AgNPs, *Dendropanax* silver nanoparticles; D-AuNPs, *Dendropanax* gold nanoparticles.

D-AgNPs and D-AuNPs induce apoptosis in A549 cells

Apoptosis, which is a process of cell death that occurs as a normal part of development, is altered in cancer cells. Previous studies have reported the ability of AgNPs and AuNPs to induce apoptosis.[26,36] We evaluated the ability of D-AgNPs alone or in combination with CK to induce cellular apoptosis based on Hoechst 33258 staining. We found that D-AgNPs alone induced changes in the nuclear morphology of many cells at 50 μg/mL, but combination treatment with 50 μg/mL of D-AgNPs with 25 μM of CK exhibited even more apoptotic bodies. Also, the D-AuNP treatment group exhibited apoptotic characteristics in only a few cells up to 50 μg/mL. In contrast, after combination

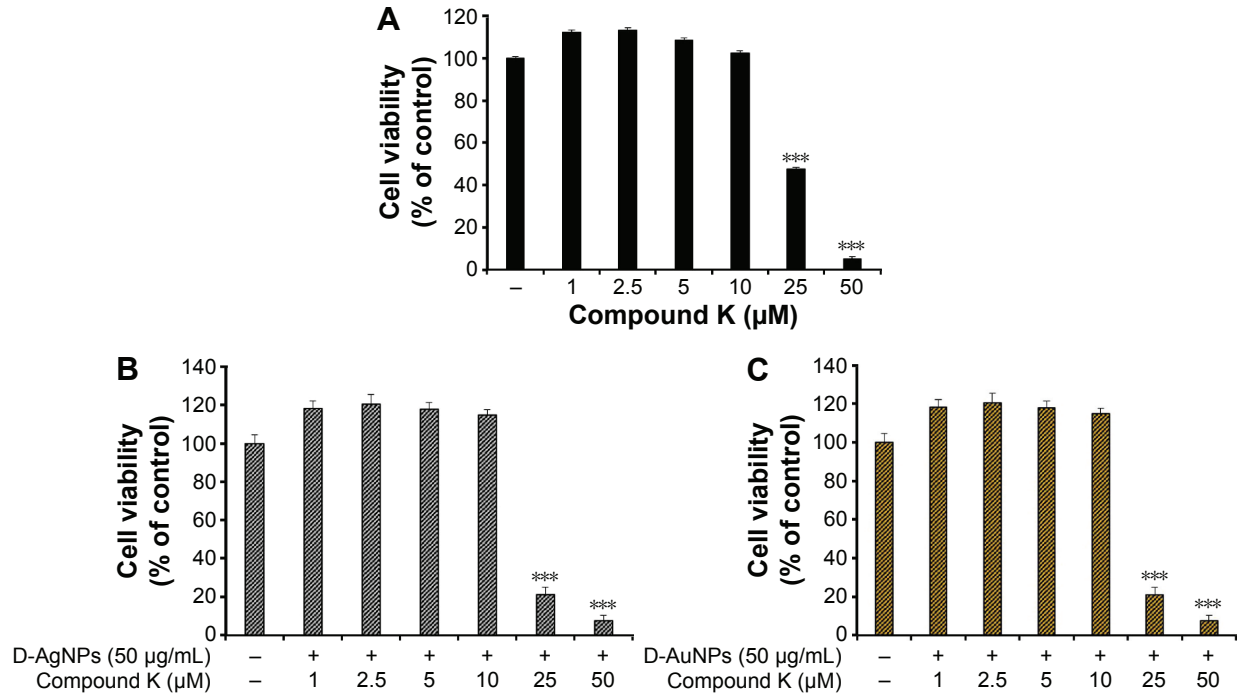

Figure 8 Synergistic effect of Compound K and D-NPs.
Notes: Cytotoxicity of CK on A549 human lung cancer cells after 48 hours of treatment (**A**). Synergistic effect of D-AgNPs (**B**) and D-AuNPs (**C**) combined with CK in a dose-dependent manner after 48 hours of treatment in A549 human lung cancer cells. Dose-dependent response. Error bars represent the standard deviation (n=3). ***$P<0.001$ versus control (untreated group). The statistical significance of differences between values was evaluated by one-way ANOVA. – indicates the absence of D-AgNPS or cmpound K and + indicates the presence of D-AgNPS or compound K in the culture medium.
Abbreviations: CK, compound K; D-AgNPs, *Dendropanax* silver nanoparticles; D-AuNPs, *Dendropanax* gold nanoparticles.

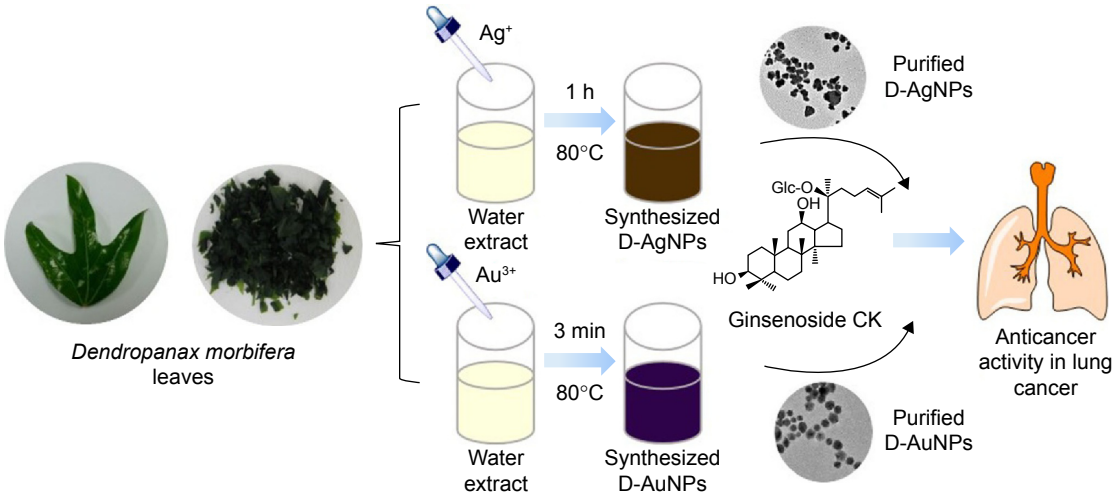

Figure 9 Schematic workflow of *D. morbifera* silver and gold nanoparticle synthesis and application.
Note: Cell apoptosis was determined by Hoechst 33258 staining.
Abbreviations: *D. morbifera, Dendropanax morbifera*; h, hour; CK, compound K; min, minutes; D-AgNPs, *Dendropanax* silver nanoparticles; D-AuNPs, *Dendropanax* gold nanoparticles.

treatment with 50 µg/mL of D-AuNPs and 25 µM CK, an increase in the number of cells with nuclei that appeared shrunken or fragmented was observed compared to that of CK or D-AuNPs alone (Figure S1). Previous studies have reported morphological characteristics such as cell shrinkage, chromatin condensation, and nuclear fragmentation as signs of cell apoptosis.[37,38] Taken together, our data showed that D-AgNPs alone can induce cell apoptosis. Also, we suggest that D-AgNPs and D-AuNPs have synergistic activity with CK on the induction of cell apoptosis.

In short, this study demonstrated the cytotoxic activity of D-AgNPs and the synergistic effect of D-AgNPs/CK and D-AuNPs/CK for the first time.

Conclusion

In this study, we report for the first time the use of a low-cost and one-step biosynthesis approach for D-AgNPs and D-AuNPs using natural herbal *D. morbifera* Léveille leaf extracts in 1 hour and 3 minutes, respectively. We demonstrated the cytotoxicity of D-AgNPs (100 µg/mL) and noncytotoxicity of D-AuNPs (100 µg/mL) in human keratinocytes (HaCaT cell line) and human lung cancer cells. Also, we examined apoptosis activities of D-AgNPs and D-AuNPs in A549 cells. The results evidence that D-AgNPs have promising anticancer property against A549 cells. Comparatively, D-AuNPs showed no cytotoxic effect in HaCaT and cancer cells, and D-AgNPs reduced the cell viability of both cell lines. Based on the results, both nanoparticles supplemented with ginsenoside CK have more synergetic anticancer effect on A549 lung cancer (Figure 9). Moreover, a fundamental analysis of D-AgNPs and D-AuNPs will support further analysis for various applications.

Acknowledgments

This research was supported by Korea Institute of Planning & Evaluation for Technology in Food, Agriculture, Forestry & Fisheries (KIPET NO: 313038-03-2-SB020), Republic of Korea.

Disclosure

The authors report no conflicts of interest in this work.

References

1. Chung IM, Kim MY, Park SD, Park WH, Moon HI. In vitro evaluation of the antiplasmodial activity of *Dendropanax morbifera* against chloroquine-sensitive strains of *Plasmodium falciparum*. *Phytother Res*. 2009;23(11):1634–1637.
2. Ahn JC, Kim SH, Kim MY, Kim OT, Kim KS, Hwang B. Seasonal variations in yields of Hwangchil lacquer and major sesquiterpene compounds from selected superior individuals of *Dendropanax morbifera* Lev. *J Plant Biol*. 2003;46(1):38–40.
3. Chung IM, Seo SH, Kang EY, Park SD, Park WH, Moon HI. Chemical composition and larvicidal effects of essential oil of *Dendropanax morbifera* against *Aedes aegypti L*. *Biochem Syst Ecol*. 2009;37(4):470–473.
4. Chung IM, Kim MY, Park WH, Moon HI. Antiatherogenic activity of *Dendropanax morbifera* essential oil in rats. *Pharmazie*. 2009;64(8):547–549.
5. Lim L, Yun JJ, Jeong JE, Wi AJ, Song H. Inhibitory effects of nano-extract from *Dendropanax morbifera* on proliferation and migration of vascular smooth muscle cells. *J Nanosci Nanotechnol*. 2015;15(1):116–119.
6. Kim W, Yoo DY, Jung HY, et al. Antioxidant effects of *Dendropanax morbifera* Leveille extract in the hippocampus of mercury-exposed rats. *BMC Complement Altern Med*. 2015;15:247.
7. Choi JH, Kim DW, Park SE, et al. Anti-thrombotic effect of rutin isolated from *Dendropanax morbifera* Leveille. *J Biosci Bioeng*. 2015;120(2):181–186.
8. Singh P, Kim YJ, Wang C, Mathiyalagan R, El-Agamy Farh M, Yang DC. Biogenic silver and gold nanoparticles synthesized using red ginseng root extract, and their applications. *Artif Cell Nanomed Biotechnol*. 2016;44(3):811–816.

9. Singh P, Kim YJ, Wang C, Mathiyalagan R, Yang DC. The development of a green approach for the biosynthesis of silver and gold nanoparticles by using *Panax ginseng* root extract, and their biological applications. *Artif Cell Nanomed Biotechnol*. 2015;44(4):1150–1157.
10. Singh P, Kim YJ, Wang C, Mathiyalagan R, Yang DC. *Weissella oryzae* DC6-facilitated green synthesis of silver nanoparticles and their antimicrobial potential. *Artif Cell Nanomed Biotechnol*. 2015;1–7. Epub 2015 Jul 23.
11. Vigneshwaran N, Kathe AA, Varadarajan PV, Nachane RP, Balasubramanya RH. Functional finishing of cotton fabrics using silver nanoparticles. *J Nanosci Nanotechnol*. 2007;7(6):1893–1897.
12. Kokura S, Handa O, Takagi T, Ishikawa T, Naito Y, Yoshikawa T. Silver nanoparticles as a safe preservative for use in cosmetics. *Nanomedicine*. 2010;6(4):570–574.
13. Martinez-Gutierrez F, Olive PL, Banuelos A, et al. Synthesis, characterization, and evaluation of antimicrobial and cytotoxic effect of silver and titanium nanoparticles. *Nanomedicine*. 2010;6(5):681–688.
14. Sukirtha R, Priyanka KM, Antony JJ, et al. Cytotoxic effect of Green synthesized silver nanoparticles using *Melia azedarach* against in vitro HeLa cell lines and lymphoma mice model. *Process Biochem*. 2012; 47(2):273–279.
15. Tian J, Wong KKY, Ho CM, et al. Topical delivery of silver nanoparticles promotes wound healing. *ChemMedChem*. 2007;2(1):129–136.
16. Mittal AK, Chisti Y, Banerjee UC. Synthesis of metallic nanoparticles using plant extracts. *Biotechnol Adv*. 2013;31(2):346–356.
17. Hyun TK, Kim MO, Lee H, Kim Y, Kim E, Kim J-S. Evaluation of anti-oxidant and anti-cancer properties of *Dendropanax morbifera* Leveille. *Food Chem*. 2013;141(3):1947–1955.
18. Moon H-I. Antidiabetic effects of dendropanoxide from leaves of *Dendropanax morbifera* Leveille in normal and streptozotocin-induced diabetic rats. *Hum Exp Toxicol*. 2011;30(8):870–875.
19. Elavazhagan T, Arunachalam KD. *Memecylon edule* leaf extract mediated green synthesis of silver and gold nanoparticles. *Int J Nanomedicine*. 2011;6:1265–1278.
20. Park Y, Hong YN, Weyers A, Kim YS, Linhardt RJ. Polysaccharides and phytochemicals: a natural reservoir for the green synthesis of gold and silver nanoparticles. *IET Nanobiotechnol*. 2011;5(3):69–78.
21. Chandran SP, Chaudhary M, Pasricha R, Ahmad A, Sastry M. Synthesis of gold nanotriangles and silver nanoparticles using *Aloe vera* plant extract. *Biotechnol Prog*. 2006;22(2):577–583.
22. Wang C, Kim YJ, Singh P, Mathiyalagan R, Jin Y, Yang DC. Green synthesis of silver nanoparticles by *Bacillus methylotrophicus*, and their antimicrobial activity. *Artif Cell Nanomed Biotechnol*. 2016;44(4): 1127–1132.
23. Singh P, Kim YJ, Singh H, Mathiyalagan R, Wang C, Yang DC. Biosynthesis of anisotropic silver nanoparticles by *Bhargavaea indica* and their synergistic effect with antibiotics against pathogenic microorganisms. *J Nanomater*. 2015;2015. Article ID 234741.
24. Lee SH, Salunke BK, Kim BS. Sucrose density gradient centrifugation separation of gold and silver nanoparticles synthesized using *Magnolia kobus* plant leaf extracts. *Biotechnol Bioprocess Eng*. 2014;19(1): 169–174.
25. Kim S, Jang Y, Han J, Chung H, Lee S, Cho K. Genetic variation and population structure of *Dendropanax morbifera* Lev.(Araliaceae) in Korea. *Silvae Genet*. 2006;55(1):7–12.
26. Kathiravan V, Ravi S, Ashokkumar S. Synthesis of silver nanoparticles from *Melia dubia* leaf extract and their *in vitro* anticancer activity. *Spectrochim Acta A Mol Biomol Spectrosc*. 2014;130:116–121.
27. Babu PJ, Sharma P, Saranya S, Bora U. Synthesis of gold nanoparticles using ethonolic leaf extract of *Bacopa monnieri* and UV irradiation. *Mater Lett*. 2013;93:431–434.
28. Jemal A, Bray F, Center MM, Ferlay J, Ward E, Forman D. Global cancer statistics. *CA Cancer J Clin*. 2011;61(2):69–90.
29. Das RK, Gogoi N, Babu PJ, Sharma P, Mahanta C, Bora U. The synthesis of gold nanoparticles using *Amaranthus spinosus* leaf extract and study of their optical properties. *Adv Mater Phys Chem*. 2012;2(4): 275–281.
30. Sankar R, Karthik A, Prabu A, Karthik S, Shivashangari KS, Ravikumar V. *Origanum vulgare* mediated biosynthesis of silver nanoparticles for its antibacterial and anticancer activity. *Colloids Surf B Biointerfaces*. 2013;108:80–84.
31. Vasanth K, Ilango K, Mohan Kumar R, Agrawal A, Dubey GP. Anticancer activity of *Moringa oleifera* mediated silver nanoparticles on human cervical carcinoma cells by apoptosis induction. *Colloids Surf B Biointerfaces*. 2014;117:354–359.
32. Suliman YAO, Ali D, Alarifi S, Harrath AH, Mansour L, Alwasel SH. Evaluation of cytotoxic, oxidative stress, proinflammatory and genotoxic effect of silver nanoparticles in human lung epithelial cells. *Environ Toxicol*. 2015;30(2):149–160.
33. Mathiyalagan R, Subramaniyam S, Kim YJ, Kim YC, Yang DC. Ginsenoside compound K-bearing glycol chitosan conjugates: synthesis, physicochemical characterization, and *in vitro* biological studies. *Carbohydr Polym*. 2014;112:359–366.
34. Mathiyalagan R, Subramaniyam S, Kim YJ, et al. Synthesis and pharmacokinetic characterization of a pH-sensitive polyethylene glycol ginsenoside CK (PEG-CK) conjugate. *Biosci Biotechnol Biochem*. 2014;78(3):466–468.
35. Yang XD, Yang YY, Ouyang DS, Yang GP. A review of biotransformation and pharmacology of ginsenoside compound K. *Fitoterapia*. 2015; 100:208–220.
36. Geetha R, Ashokkumar T, Tamilselvan S, Govindaraju K, Sadiq M, Singaravelu G. Green synthesis of gold nanoparticles and their anticancer activity. *Cancer Nanotechnol*. 2013;4(4–5):91–98.
37. Kerr JF, Wyllie AH, Currie AR. Apoptosis: a basic biological phenomenon with wide-ranging implications in tissue kinetics. *Br J Cancer*. 1972;26(4):239–257.
38. Wyllie AH, Kerr JF, Currie AR. Cell death: the significance of apoptosis. *Int Rev Cytol*. 1980;68:251–306.

Supplementary material

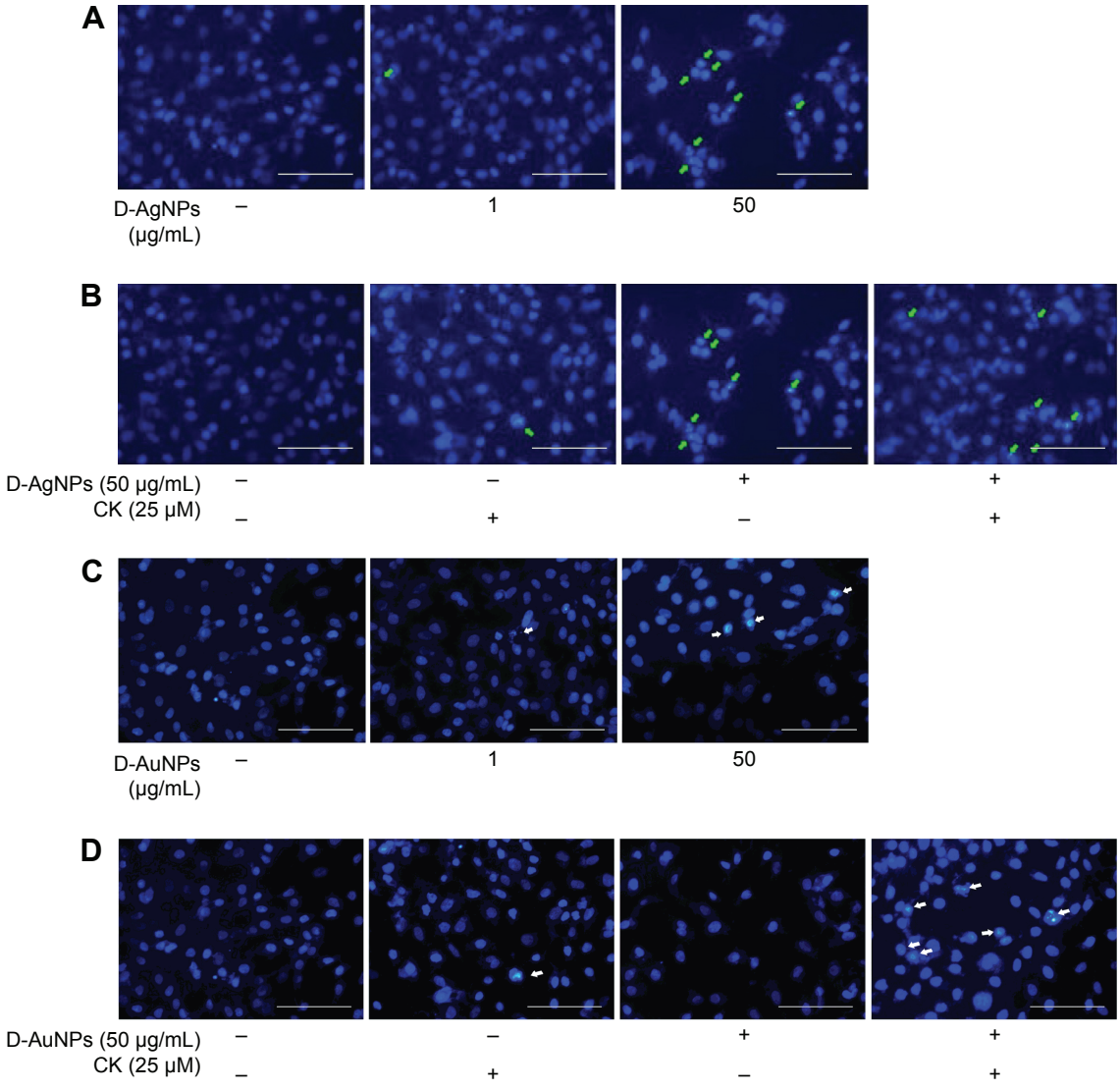

Figure S1 Cell apoptosis determined by Hoechst 33258 staining.

Notes: Morphological changes in A549 cells treated with (**A**) D-AgNPs, (**B**) CK combination with D-AgNPs, (**C**) D-AuNPs, and (**D**) CK combination with D-AuNPs for 48 hours and stained with Hoechst 33258 dye. A synergistic effect induced apoptosis and morphological changes in A549 cells. Apoptotic cells are indicated with an arrow. The magnification scale is 400×. Scale bars are 10 μm.

Abbreviations: CK, compound K; D-AgNPs, *Dendropanax* silver nanoparticles; D-AuNPs, *Dendropanax* gold nanoparticles.